Journal of Hydrology 524 (2015) 367–377

Contents lists available at ScienceDirect

Journal of Hydrology

journal homepage: www.elsevier.com/locate/jhydrol

Characterization of alluvial formation by stochastic modelling of paleo-fluvial processes: The concept and method

Zhenjiao Jiang [a,b,*], Gregoire Mariethoz [c,d], Troy Farrell [e], Christoph Schrank [b,f], Malcolm Cox [b]

[a] Key Laboratory of Groundwater Resources and Environment, Ministry of Education, College of Environment and Resources, Jilin University, ChangChun 130021, China
[b] School of Earth, Environmental & Biological Sciences, Queensland University of Technology, Brisbane, QLD 4001, Australia
[c] Institute of Earth Surface Dynamics, University of Lausanne, 1015 Lausanne, Switzerland
[d] School of Civil and Environmental Engineering, University of New South Wales, Sydney, NSW 2052, Australia
[e] School of Mathematical Sciences, Queensland University of Technology, Brisbane, QLD 4001, Australia
[f] School of Earth and Environment, The University of Western Australia, Crawley 6009, Australia

ARTICLE INFO

Article history:
Received 24 August 2014
Received in revised form 31 January 2015
Accepted 2 March 2015
Available online 10 March 2015
This manuscript was handled by Peter K. Kitanidis, Editor-in-Chief, with the assistance of Markus Tuller, Associate Editor

Keywords:
Process-based model
Alluvial reservoir
Perturbation theory
Spectral approach

SUMMARY

Modelling fluvial processes is an effective way to reproduce basin evolution and to recreate riverbed morphology. However, due to the complexity of alluvial environments, deterministic modelling of fluvial processes is often impossible. To address the related uncertainties, we derive a stochastic fluvial process model on the basis of the convective Exner equation that uses the statistics (mean and variance) of river velocity as input parameters. These statistics allow for quantifying the uncertainty in riverbed topography, river discharge and position of the river channel. In order to couple the velocity statistics and the fluvial process model, the perturbation method is employed with a non-stationary spectral approach to develop the Exner equation as two separate equations: the first one is the mean equation, which yields the mean sediment thickness, and the second one is the perturbation equation, which yields the variance of sediment thickness. The resulting solutions offer an effective tool to characterize alluvial aquifers resulting from fluvial processes, which allows incorporating the stochasticity of the paleoflow velocity.

1. Introduction

Rivers are one of the most dynamic external forces interacting with and modifying the Earth's surface. Sediment erosion and deposition in rivers (fluvial processes) affect the geomorphic evolution of land surface and basin stratigraphy. Various models have been developed over the past decades to quantitatively describe fluvial processes, including geostatistical models that mimic the final results of fluvial processes statistically, and process-based models that quantify the physics of fluid and sediment transport (e.g. Koltermann and Gorelick, 1996; Paola, 2000; Van De Wiel et al., 2011). Geostatistical methods predict unknown data by interpolation based on probabilistic models inferred from measured data. These methods can be conditioned to the measured information, but their applicability is often limited due to sparse data. In contrast, process-based models which describe the mechanics of fluvial processes can be used to simulate the lithology distribution in the absence of measurements (Li et al., 2004; Tetzlaff, 1990).

The Exner model is a classical process-based description of fluvial processes, which is based on a mass balance of sediment transport in the river and sediment accumulation on the riverbed (Exner, 1925; Leliavsky, 1955). It was generalized by Paola and Voller (2005) to consider the influence of tectonic uplift and subsidence, soil formation and creep, compaction and chemical precipitation and dissolution. For a wide range of specific problems, such as short- or long-term riverbed evolution, a mass balance equation can be extracted from the general Exner equation by combining and dropping negligible terms.

Fluvial process models based on the general Exner equation are widely used. Several types of such models are available. In the convective model (Davy and Lague, 2009; Paola and Voller, 2005), the sediment flux and accumulation at the position of interest is assumed to be controlled by the upstream landscape features and sediment input. The diffusion model (Paola et al., 1992; Paola and Voller, 2005) simulates influences of both upstream and downstream locations on the target positions. In addition, the fractional model (Voller et al., 2012) accounts for non-local upstream and downstream influences.

* Corresponding author at: Key Laboratory of Groundwater Resources and Environment, Ministry of Education, College of Environment and Resources, Jilin University, ChangChun 130021, China. Tel.: +86 13756261306.
E-mail address: jiangzhenjiao@hotmail.com (Z. Jiang).

http://dx.doi.org/10.1016/j.jhydrol.2015.03.007
0022-1694/

Nomenclature

Symbol	Definition
β	deposition coefficient, L/T
C_d	dimensionless drag coefficient
D	deposition rate of sediment, L/T
$dZ_v(\kappa)$	complex Fourier amplitude of flow velocity
Δt	time step, T
Δx	length of discretized segment, L
E	erosion rate of sediment, L/T
γ	erosion efficiency coefficient, $L^{2.5}\,T^2/M^{1.5}$
H	river depth, L
κ	magnitude of the wave number vector
λ	correlation scale of the flow velocity, L
p	probability of the channel occurrence
ϕ	transfer function between v and η
ϕ^*	conjunction of ϕ
φ	porosity of deposited sediment
$q_s(t)$	sediment input from the river source, L
ρ_f	density of water, M/L^3
$s_{vv}(\kappa)$	spectral density function of flow velocity
t	time, T
v	stream velocity, L/T
W_f	width of fluvial trace, L
W_c	width of river channel, L
x	distance along the stream from its origin, L
η	sediment load in the river, L^3/L^2
σ_M^2	variance of the quantity M
z	sediment thickness, L

In these fluvial process models (FPM), the flow velocity is the key input parameter. The velocity can be resolved by a fluid dynamics model (FDM) based on the Navier–Stokes equations (e.g. Gonzalez-Juez et al., 2009; Necker et al., 2005). Approaches that couple FPM and FDM can yield a detailed description of fluvial processes and channel evolution. However, these are mostly limited to controlled laboratory settings. At the catchment scale, a coupled FPM–FDM has been applied in two-dimensional planes where the vertical velocity variation has been neglected (Koltermann and Gorelick, 1992). Fully-coupled modelling of the fluvial processes and fluid dynamics, however, is still a challenge, because applying the FDM requires precise knowledge of the initial and flow boundary conditions, which are generally not available (e.g. Koltermann and Gorelick, 1992; Lesshafft et al., 2011; Simpson and Castelltort, 2006).

Due to these difficulties, the determination of flow velocity is often uncertain. Therefore, a trend in the past decades has been to develop stochastic fluvial process models that account for the stochasticity in the river discharge (e.g. Lague, 2014; Molnar et al., 2006; Tucker and Bras, 2000), and the stochasticity of particle motion (e.g. Furbish et al., 2012; Roseberry et al., 2012).

In this paper, we pursue a similar stochastic approach by developing the convective FPM (Davy and Lague, 2009), to account for the uncertainties in factors that can be represented by the statistics of flow velocity. These factors include riverbed topography, river discharge and river channel position in the fluvial trace. The velocity in the model is characterized by a stochastic description consisting of an ensemble mean component and a perturbation component. The model relates the statistics of the velocity with the statistics of sediment load in the river and of sediment thickness on the riverbed.

This study is organized as follows: Section 2 introduces the convective FPM and the stochastic formulation employing the perturbation method. Section 3 derives the analytical solutions for the sediment load and sediment thickness. The algorithmic implementation is summarized in Section 4 and Section 5 applies the stochastic model to a synthetic case.

2. Governing equations

2.1. Mass balance equation

The mass balance describing fluvial processes is expressed as two separate equations (Davy and Lague, 2009; Paola and Voller, 2005). The first one describes sediment transport in the river:

$$\frac{\partial \eta(x,t)}{\partial t} + \frac{\partial v(x,t)\eta(x,t)}{\partial x} - E(x,t) + D(x,t) = 0, \tag{1}$$

and the second one describes sediment accumulation on the riverbed:

$$\frac{\partial z(x,t)}{\partial t} = \frac{1}{1-\varphi}[D(x,t) - E(x,t)]. \tag{2}$$

Expressions for E (erosion rate) and D (deposition rate) are given in Appendix B. A list of notation is available at the end.

The flow velocity (v) is one of the key parameters in Eqs. (1) and (2), which can be modelled by Navier–Stokes equation (Necker et al., 2005) or simply described by the Manning formula (e.g. Lague, 2010; Le Méhauté, 1976) (Appendix A). However, the application of Eqs. (1) and (2) to reproduce a geological formation often presents uncertainties, because the factors influencing v such as paleotopography and paleohydrology are difficult to determine. It is therefore necessary to develop Eqs. (1) and (2) as stochastic equations that contains the information on the uncertainty of v. Due to the complexity of the factors influencing alluvial sedimentary processes, we deliberately chose to make the following simplifying assumptions:

(1) Chemical precipitation and dissolution, and the abrasion of the sediment particles are not considered.
(2) One-dimensional convective Exner model in Eqs. (1) and (2) is flexible for the modelling river morphodynamics in an inland sedimentary basin. The influences of sediment particle diffusion and the downstream boundary on sediment transport and accumulation are neglected (Zolezzi and Seminara, 2001). In the near-shore environment, where the downstream boundary has significant influence on the sedimentary processes, it would be worthwhile to use the diffusive Exner equation, which is not discussed in this study.
(3) We focus on the uncertainty in sediment transport and accumulation induced by the velocity fluctuation, but the uncertainty relating to the sediment load fluctuation attributed, for example, to the tributaries, is beyond the scope of this study.

2.2. Mass balance equation revisited

Eqs. (1) and (2) are nonlinear partial differential equations, which are solved numerically. River channels are discretised into N segments with $N+1$ nodes, and v is assumed to be constant within each segment (Lanzoni and Seminara, 2002). Eqs. (1) and (2) are then rewritten as:

$$\frac{\partial \eta(x_k,t)}{\partial t} + v_k \frac{\partial \eta(x_k,t)}{\partial x_k} - E_k + D_k = 0, \tag{3}$$

and

$$\frac{\partial z_k(t)}{\partial t} = \frac{1}{1-\varphi_k}(D_k - E_k), \tag{4}$$

where k indicates the k-th segment ($k = 1, 2, \ldots N$), x_k is the coordinate of the k-th segment.

The perturbation method is used to couple the uncertainty of v_k in Eqs. (3) and (4), considering the quantities in the equation as a sum of the ensemble mean and a perturbation surrounding the mean (Holmes, 2013):

$$\begin{aligned}
&v_k = \bar{v}_k + v'_k, \overline{v'_k} = 0, \sigma^2_{v_k} = \overline{v'_k v'_k},\\
&D_k = \overline{D_k} + D'_k, \overline{D_k}' = 0,\\
&E_k = \overline{E}_k + E'_k, \overline{E'_k} = 0,\\
&\eta(x_k,t) = \bar{\eta}(x_k,t) + \eta'(x_k,t), \overline{\eta'}(x_k,t) = 0, \sigma^2_{\eta}(x_k,t) = \overline{\eta'(x_k,t)\eta'(x_k,t)},\\
&z_k(t) = \bar{z}_k(t) + z'_k(t), \overline{z'_k}(t) = 0, \sigma^2_{z_k}(t) = \overline{z'_k(t) z'_k(t)},
\end{aligned} \tag{5}$$

where the bar indicates ensemble mean of these quantities, the prime indicates a zero-mean perturbation.

Substituting Eqs. (5) in (3) gives:

$$\begin{aligned}
&\frac{\partial[\bar{\eta}(x_k,t) + \eta'(x_k,t)]}{\partial t} + (\bar{v}_k + v'_k)\frac{\partial[\bar{\eta}(x_k,t) + \eta'(x_k,t)]}{\partial x_k}\\
&- \overline{E}_k - E'_k + \overline{D}_k + D'_k = 0.
\end{aligned} \tag{6}$$

Taking the ensemble mean on both sides of Eq. (6) to remove the first-order perturbation terms, leaves a mean equation:

$$\frac{\partial \bar{\eta}(x_k,t)}{\partial t} + \bar{v}_k\frac{\partial \bar{\eta}(x_k,t)}{\partial x_k} + \overline{v'_k\frac{\partial \eta'(x_k,t)}{\partial x_k}} - \bar{E}_k + \bar{D}_k = 0. \tag{7}$$

Subtracting Eq. (7) from (6) yields the perturbation equation:

$$\frac{\partial \eta'(x_k,t)}{\partial t} + \bar{v}_k\frac{\partial \eta'(x_k,t)}{\partial x_k} + v'_k\frac{\partial \bar{\eta}(x_k,t)}{\partial x_k} - E'_k + D'_k = 0. \tag{8}$$

Eq. (8) can be rewritten as:

$$\frac{\partial \eta'(x_k,t)}{\partial t} + \bar{v}_k\frac{\partial \eta'(x_k,t)}{\partial x_k} - w_{uk}v'_k = 0, \tag{9}$$

where $w_{uk} = w_{sk} + w_{dk} + w_{ek}$ represents the influence of the velocity changes on the sediment load via sediment flux ($w_{sk} = -\partial\bar{\eta}(x_k,t)/\partial x_k$), deposition ($w_{dk}$) and erosion ($w_{ek}$). w_{dk} represents the influence of $v_{k'}$ on $\eta_{k'}$ via altering D_k. Expressions for w_{dk} and w_{ek} are given in Appendix B. According to Eq. (B7), $v_{k'}$ does not directly induce D_k changes (Winterwerp and Van Kesteren, 2004), and therefore, $w_{dk} = 0$. w_{ek} satisfies:

$$w_{ek} = \gamma_k(c_{dk}\rho_f)^{1.5}(3\bar{v}_k^2 + \sigma^2_{v_k}), \tag{10}$$

Similarly, making use of Eq. (5) in Eq. (4) yields a mean equation:

$$\frac{\partial \bar{z}_k(t)}{\partial t} = \frac{1}{1-\varphi_k}(\overline{D}_k - \overline{E}_k), \tag{11}$$

and a perturbation equation:

$$\frac{\partial z'_k(t)}{\partial t} = \frac{1}{1-\varphi_k}(D_k{}' - E'_k), \tag{12}$$

Eqs. (7), (9), (11) and (12) form the governing equations of the stochastical fluvial process-based model (SFPM). The governing Eqs. (7) and (11) are solved for $\bar{\eta}$ and $\bar{z}$, given certain boundary conditions. Relationships between η', z' and v' from Eqs. (9) and (12) are expressed as functions describing the variances of sediment load and streambed height, namely $\sigma^2_{\eta} \sim f_{\eta}(\sigma^2_{v})$ and $\sigma^2_{z} \sim f_{z}(\sigma^2_{v})$. The solutions for σ^2_{η}, $\bar{\eta}$, σ^2_{z} and $\bar{z}$ are derived in Section 3.

2.3. The concept of ensemble velocity

In Section 2.2, the velocity in Eqs. (1) and (2) has been replaced by the statistics of the ensemble velocity, which is quantified by a mean velocity and a perturbation (or variance). The ensemble velocity is not limited to represent the velocity variation within the river channel, but can describe the possible velocities at a position in the fluvial trace within the sedimentation period (Fig. 1a–c). When the river channel intersects a given position P, the ensemble velocity represents the velocity in the river channel, perturbed by the uncertainties in riverbed slope, bank friction, flow rate and flooding. When the river channel moves away, there is no erosion and deposition at the given position and the flow velocity is zero. The ensemble velocity at any position in the fluvial trace includes the possible velocities in the river channel, and the zero values related to the absence of an active channel (Fig. 1c and d). The probability distribution of ensemble velocity at the given position is allowed to be skewed, and the skewness decreases with the increasing ratio between widths of the channel and fluvial trace (Fig. 1d) (Appendix D). In other words, the smaller the fraction of a fluvial trace occupied by active river channels, the larger the probability of encountering zero flow velocity.

The variability of velocity related to channel movement occurs slowly, at a different time scale than the velocity changes in the river channel. However, these two time scales of velocity variations can be considered coevally in the statistics of ensemble velocity (Furbish et al., 2012; Gibbs, 2010), because the statistics of ensemble velocity is estimated at a fixed time over all possible values of velocity (see Appendix A).

3. Semi-analytical solutions

3.1. Solution for the variance of sediment load (σ^2_{η})

This section derives the solution for σ^2_{η} from Eq. (9), using the nonstationary spectral method, which is based on a Fourier transform. The Fourier–Stieltjes representation of the random process η' is (Gelhar and Axness, 1983; Li and McLaughlin, 1995; Ni et al., 2010):

$$\eta'(x_k,t) = \int_{-\infty}^{+\infty} \varphi(x_k,t,\kappa)dZ_v(\kappa), \tag{13}$$

and v' is represented by:

$$v'_k = \int_{-\infty}^{+\infty} e^{i\kappa x_k}dZ_v(\kappa), \tag{14}$$

where $i = \sqrt{-1}$.

Substituting Eqs. (13) and (14) in Eq. (9) gives:

$$\frac{\partial \phi(x_k,t,\kappa)}{\partial t} + \bar{v}_k\frac{\partial \phi(x_k,t,\kappa)}{\partial x_k} - w_{uk}e^{i\kappa x_k} = 0. \tag{15}$$

At the source of the river, η' is determined by the natural boundary condition, which is unrelated to the flow velocity:

$$\eta'(0,t) = 0. \tag{16}$$

The Fourier representation of Eq. (16) implies:

$$\phi(0,t,\kappa) = 0. \tag{17}$$

Solving Eq. (15) subject to Eq. (17) results in a general solution for $\phi(x,t,\kappa)$ at end of each segment (details in Appendix C):

$$\phi(x_m,t,\kappa) = \left(\frac{1}{i\kappa}e^{i\kappa\Delta x} - \frac{1}{i\kappa}\right)\sum_{k=1}^{m}\left(\frac{w_{uk}}{\bar{v}_k}\right), \tag{18}$$

where m is the index of node ($m = 0, 1, 2, \ldots, N$).

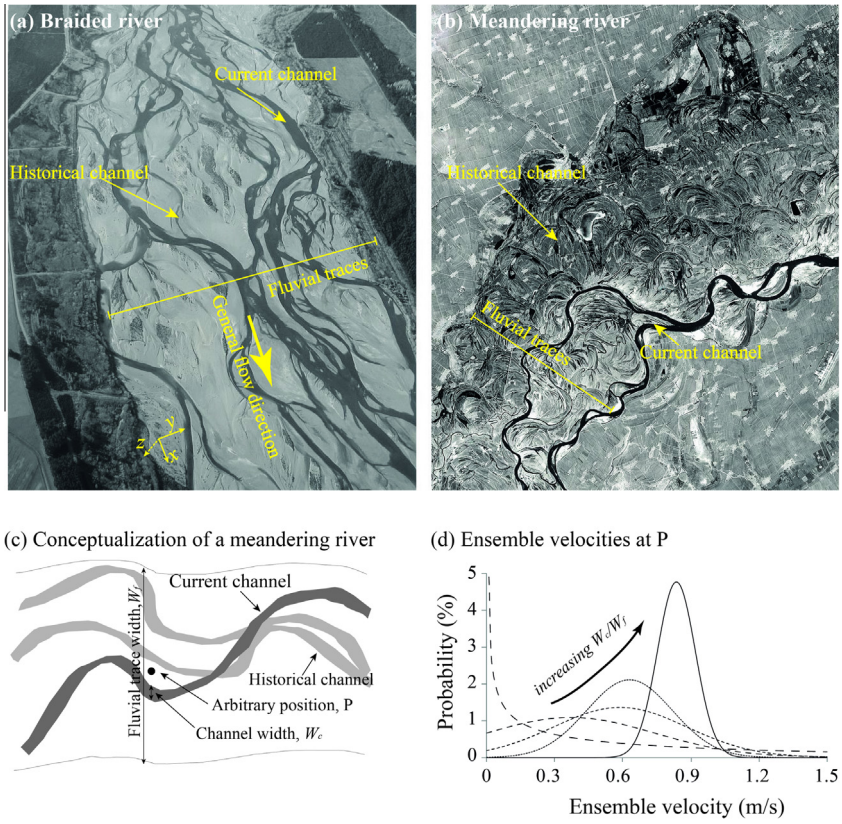

Fig. 1. Satellite images of the river channel and fluvial traces in (a) braided and (b) meandering rivers. (c) Conceptualization of a meandering river and (d) the possible probability distributions of the ensemble velocity at a given position in the fluvial trace with different ratio between widths of channel and fluvial trace.

Once ϕ is expressed analytically, the variance of η can be calculated as:

$$\begin{aligned}\overline{\eta'\eta'} &= \int_{-\infty}^{\infty} \phi(x,t,\kappa)\cdot\phi^*(x,t,\kappa)s_{vv}(\kappa)d\kappa,\\ \overline{\eta' v'} &= \int_{-\infty}^{\infty} e^{i\kappa x}\cdot\phi^*(x,t,\kappa)s_{vv}(\kappa)d\kappa,\\ \overline{v'\frac{\partial\eta'}{\partial x}} &= \int_{-\infty}^{\infty} e^{i\kappa x}\frac{\partial\phi^*(x,t,\kappa)}{\partial x}s_{vv}(\kappa)d\kappa,\end{aligned} \tag{19}$$

Commonly used spectral density functions for the natural quantities include the exponential model and Gaussian model, which are the Fourier transform of the covariance function of v' between two positions with variable spatial separations (Dagan, 1989; Zhu and Satish, 1999). Both models present slight differences, mainly for small lags: for an exponential model, the covariance function drops immediately with separation distance above zero, but the covariance function for Gaussian models is more continuous near the origin. The Gaussian model is more nonlinear, and therefore does not lead to a closed expression if used in Eq. (19). Here we use the exponential model:

$$s_{vv}(\kappa) = \frac{2\kappa^2\sigma_v^2\lambda^3}{\pi(1+\kappa^2\lambda^2)^2}, \tag{20}$$

The upstream flow velocity affects the downstream velocity, hence λ at different locations on the river is the flow distance ($\lambda = x$).

Substituting Eqs. (18) and (20) into (19) yields the closed-form expressions for the variance of sediment load (σ_η^2) and covariance between sediment load and velocity ($\sigma_{\eta v}$):

$$\begin{aligned}\sigma_{\eta_m}^2 &= \overline{\eta_m'\eta_m'} = 2\lambda_m^2\left(1-\tfrac{\lambda_m+\Delta x}{\lambda_m}e^{-\frac{\Delta x}{\lambda_m}}\right)\left[\sum_{k=1}^{m}\left(\tfrac{w_{uk}}{v_k}\right)\right]^2\sigma_{v_m}^2,\\ \sigma_{\eta_m v_m} &= \overline{\eta_m' v_m'} = \left(x_m e^{-\frac{x_m}{\lambda_m}} - x_{m-1}e^{-\frac{x_{m-1}}{\lambda_m}}\right)\sum_{k=1}^{m}\left(\tfrac{w_{uk}}{v_k}\right)\cdot\sigma_{v_m}^2,\end{aligned} \tag{21}$$

where $\sigma_\eta^2 = 0$ if $\lambda = 0$, which satisfies the boundary condition in Eq. (16).

Eq. (21) suggests that the impact of v' on η' (or σ_η^2) is accumulated from upstream to downstream, as both λ and the coefficient term $\sum_{k=1}^{m}\left(\frac{w_{uk}}{v_k}\right)$ increase with the distance from the river source. We define an exaggeration factor from Eq. (21): $c = 2\lambda^2\left(1-\frac{\lambda+\Delta x}{\lambda}e^{-\frac{\Delta x}{\lambda}}\right)$, which increases with λ (also the distance to river source, x) (Fig. 2). This indicates that with an increase in x, the influence of the upstream situation on the downstream (η') is accumulated more and more significantly, but not infinitely. In the example of Fig. 2, after x exceeds 10 m (Δx is given as 1.0), the exaggeration factor approaches a constant.

In addition, the second-order perturbation term in Eq. (7) becomes:

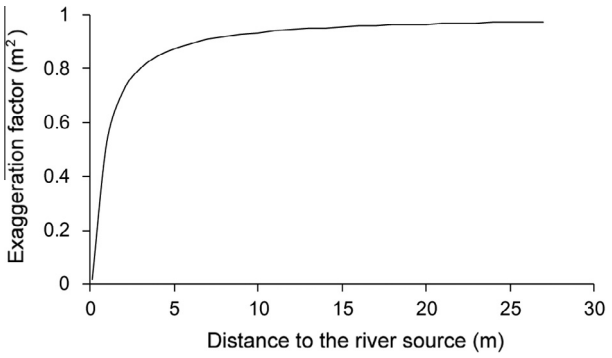

Fig. 2. The exaggeration factor related to the upstream influence increases with the distance to the river source.

$$\overline{v'_m \frac{\partial \eta'_m}{\partial x}} = \frac{w_{um}}{\bar{v}_m}\left(1 - \frac{x_m}{\lambda_m}\right) e^{-\frac{x_m}{\lambda_m}} \sigma^2_{v_m}, \tag{22}$$

which is zero because $\lambda_m = x_m$.

3.2. Solution for the mean sediment load

The mean sediment load ($\bar{\eta}$) can be solved from Eq. (7). This equation is similar to Eq. (15), which is solved as a traditional Cauchy problem subject to the boundary condition:

$$\eta(0, t) = q_s(t), \tag{23}$$

The detailed derivation is similar to the processes in Appendix C, and the interested reader can also refer to Hadamard (2003).

As a result, the sediment load at each node m can be written as:

$$\bar{\eta}_m = \sum_{k=1}^{m} \bar{E}_k \frac{\Delta x_k}{\bar{v}_k} + q_s\left(t - \sum_{k=1}^{m} \frac{\Delta x_k}{\bar{v}_k}\right) - \sum_{k=1}^{m} \bar{D}_k \frac{\Delta x_k}{\bar{v}_k}. \tag{24}$$

Eq. (24) suggests that $\bar{\eta}$ at x_m is attributed to q_s from the river source and the erosion over a distance x_m, which is expressed as the term, $\sum_{k=1}^{m} \bar{E}_k \frac{\Delta x_k}{\bar{v}_k} + q_s\left(t - \sum_{k=1}^{m} \frac{\Delta x_k}{\bar{v}_k}\right)$. This term is here defined as the potential load. The potential load decreases to $\bar{\eta}$ due to the deposition along the flow path by $\sum_{k=1}^{m} \bar{D}_k \frac{\Delta x_k}{\bar{v}_k}$.

3.3. Solution for the mean and variance of sediment thickness

Sediment is accumulated on the riverbed due to deposition and removed from the riverbed due to erosion. The mean and perturbation of sediment thickness over time step Δt (Eqs. (11) and (12)) can be rewritten as:

$$\bar{z}_m = \frac{1}{1 - \varphi_m}[\bar{D}_m - \bar{E}_m]\Delta t, \tag{25}$$

and

$$z'_m = \frac{1}{1 - \varphi_m}[D'_m - E'_m]\Delta t. \tag{26}$$

Furthermore, using expressions for E' and D' (Eq. (B5) and (B10) in Appendix B) in the perturbation Eq. (26) leads to the variance of sediment thickness:

$$\sigma^2_{z_m} = \overline{z'_m z'_m} = \frac{1}{(1 - \varphi_m)^2} \overline{\left[\frac{\beta_m}{H_m}\eta'_m - w_{em} v'_m\right]^2} \Delta t^2, \tag{27}$$

which is rewritten as:

$$\sigma^2_{z_m} = \frac{1}{(1 - \varphi_m)^2}\left[\left(\frac{\beta_m}{H_m}\right)^2 \sigma^2_{\eta_m} - 2 w_{em} \frac{\beta_m}{H_m} \sigma_{\eta v_m} + w^2_{em} \sigma^2_{vm}\right] \Delta t^2, \tag{28}$$

Eq. (28) suggests that the fluctuation of the sediment thickness on the riverbed is attributed to the perturbation of flow velocity ($\sigma^2_{v_m}$) and the induced perturbation of sediment load ($\sigma^2_{\eta_m}$). Both $\sigma^2_{v_m}$ and $\sigma^2_{\eta_m}$ affect $\sigma^2_{z_m}$ via the deposition and erosion processes, which are mathematically quantified in Eq. (27).

4. Algorithm

The algorithmic implementation of the model described in Section 3 is given below, for the reproduction of a geological profile:

(1) Select a line parallel with the general river flow direction.
(2) Discretise the selected line into N segments.
(3) Calibrate the spatial distribution of $\bar{v}$ and σ^2_v according to the river discharge, riverbed slope, and river channel position (an example is given in Appendix A).
(4) The sedimentary period is divided into limited numbers of time steps with the magnitude of Δt. Within each selected time step, the flow velocity, deposition rate and erosion rate are assumed to be constant.
(5) Assess $\bar{E}_k$ (Eq. (B4)) and w_{ek} (Eq. (B5)) for each segment ($k = 1, 2 \ldots N$).
(6) Calculate the time interval $\left(\frac{x_k}{\bar{v}_k}\right)$ for river flow through each segment.
(7) Calculate the potential $\bar{\eta}_m$ at each node m ($m = 0, 1, \ldots N$) as the sum of entrapped sediment and sediment input (Eq. (24));
(8) Calculate the real $\bar{\eta}_m$ in Eq. (24) after deposition of $\sum_{k=1}^{m} \bar{D}_k \frac{x_k}{\bar{v}_k}$ for node m. In detail, at the river source ($m = 0$), the sediment load ($\bar{\eta}_0$) is the sediment input (q_s). The deposition rate ($\bar{D}_1$) for the first segment is calculated by using $\bar{\eta}_0$ in Eq. (B9).

For the first node ($m = 1$), the potential $\bar{\eta}_1$ is the sum of the erosion over the length of the first segment plus the sediment input. However, the real $\bar{\eta}_1$ should remove the deposition volume over the first segment (deposition rate is $\bar{D}_1$ and deposition period is $\frac{x_1}{\bar{v}_1}$). The deposition rate ($\bar{D}_2$) for the second segment is calculated by using $\bar{\eta}_1$ in Eq. (B9).

For the m-th node, the potential load is the sum of erosion over a distance of $\sum_{k=1}^{m} x_k$ plus the sediment input from river source, and the real load needs the removal of a deposition volume $\sum_{k=1}^{m} \bar{D}_k \frac{x_k}{\bar{v}_k}$.

(9) Sediment thickness ($\bar{z}_m$) is recorded simultaneously with the calibration of $\bar{D}_m$ and $\bar{E}_m$ according to the mean Eq. (25).
(10) $\sigma^2_{\eta_m}$ is estimated by Eq. (21), while $\sigma^2_{z_m}$ is calculated by Eq. (28).
(11) When the computation time increases by one time step (Δt), input new river discharge. In addition, the riverbed slope may change significantly due to the sediment accumulation on the riverbed. Go back to step (3) to recalculate the velocity in space.
(12) Repeat the steps 4–13 until the total computation time becomes larger than the target simulation time. Finally, $\bar{z}_m$ and $\sigma^2_{z_m}$ calibrated over each Δt are summed up as the final sediment thickness and variance.

In addition, in order to simulate the spatial distribution of different lithologies, the transport and accumulation of sediments of multiple grain sizes are modelled based on the exhausted deposition assumption, involving that fine-grain sediments can only be deposited after the coarse-grain sediments are exhausted (Paola et al., 1992). At the end of each time step, the deposited lithology is recorded together with $\bar{z}$.

5. A synthetic case study

The major contribution of the proposed stochastic fluvial model is that it can yield both mean sediment thickness ($\bar{z}$) and variance (σ_z) resulting from the uncertain flow velocity. A synthetic example is used to illustrate the approach, with the following setting:

(1) The sediment input, q_s, from the river source is assumed to be a constant equal to 0.0001 m, which is unrelated to the river discharge Q (Viparelli et al., 2011).
(2) The streamwise variation of Q is neglected assuming that within the section of interest, there are no major tributaries

and no significant water loss induced by infiltration and evaporation.
(3) Only one type of sediment (sand) is considered.
(4) The deposited sand can be eroded, but the underlying bedrock is assumed to be non-erodible.

The coefficients for the sediment and fluid properties are given in Table 1 according to Cornelis et al. (2004) and Viparelli et al. (2011).

Moreover, the input parameters include the riverbed slope (S), river discharge (Q) and the width of the fluvial trace (W_f), which are used to infer the spatial distribution of velocity statistics. The selection of these parameters refers to the geomorphology of many inland rivers in Queensland, Australia, such as Thomson River and Alice River (Australia Government, http://watermonitoring.derm.qld.gov.au/host.htm).

The longitudinal profile of the riverbed is assumed to have an exponential shape, which represents the sedimentary environment varying from hill to coastal plain (Fig. 3b). The fluvial processes are modelled for a river length of 10,000 m. The river is discretised into 1000 segments of 10 m. Both river depth (H) and width (W_c) increase from upstream to downstream given the constant Q of 50 m^3/s in space (Fig. 1a). The width of fluvial trace (W_f) is given as 50 m.

The variation of velocity in the river channel is assumed to follow a normal distribution. Hence, the variance of velocity and mean values in the river channel satisfy $\sigma^2_{v_{ck}} = 0.26 v^2_{ck}(x,t)$ (Cox and Hinkley, 1979), where v_c results from the Manning equation in Eq. (A1). Furthermore, with regard to the possibility of channel occurrence (p) within the range of fluvial trace, the mean and variance of ensemble velocity used in this synthetic case are calibrated by (as shown in Appendix A):

$$\bar{v}_k = p_k \cdot v_{ck}, \tag{29}$$

and

$$\sigma^2_{v_k} = p_k \sigma^2_{v_{ck}} + [1 - p_k][2 - p_k] v^2_{ck}, \tag{30}$$

where $p = W_c/W_f$. As a consequence, the spatial distribution of the variance and mean of ensemble velocity herein decreases streamwise (Fig. 4).

The model evolves in time with increments of 100 years. The resulting mean sediment thickness ($\bar{z}$) is represented in Fig. 5a. The deposition rate ($\overline{D}$) reduces along the river flow direction with $\bar{\eta}$, as deposition keeps occurring. The erosion rate ($\overline{E}$) reduces along the river flow direction due to the decrease of $\bar{v}$ and σ^2_v (Appendix B). However, the decreasing $\overline{D}$ and $\overline{E}$ play reverse roles on $\bar{z}$, as deposition increases $\bar{z}$ and erosion decreases $\bar{z}$.

This results in a non-monotonic pattern of $\bar{z}$, which increases with the distance to the river source at the upstream part of the river. After peaking to 2.2 m at about 2000 m, $\bar{z}$ decreases along the river flow at the downstream part of the river.

This pattern of mean sediment thickness, induced by the coupling of deposition and erosion processes, is comparable with the results of laboratory experiments by Cui et al. (2003) and Sklar et al. (2009).

It is interesting that standard deviation of sediment thickness (σ_z) does not decrease with $\bar{v}$ or σ^2_v (Fig. 6), and is highly non-monotonic in space (Fig. 5b), which is explained as follows.

The geometries of the channel, fluvial traces and riverbed determine the spatial distribution of $\bar{v}$ and σ^2_v, which then affect the sedimentary processes via the deposition and erosion of sediment. σ_z is composed of deposition perturbation ($D' = \frac{\varepsilon_S}{\bar{H}}\eta'$) and erosion perturbation ($E' = w_{em} v_m'$) (Eq. (27)). The contrast between deposition perturbation and erosion perturbation is illustrated in Fig. 7, where the deposition factor is $f_D = D'/(D' + E')$, while the erosion factor is $f_E = E'/(D' + E')$. As a result, f_E reduces streamwise due to

Table 1
Input parameters used in fluvial process modelling (definitions in Appendix A and B).

Coefficients	Value
Conversion factor, c_f, $m^{1/3}/s$	1.0
Concentration coefficient, k_d, –	3×10^{-5}
Density of sediment, ρ_s, kg/m^3	2700
Density of water, ρ_f, kg/m^3	1000
Drag coefficient, c_d, –	0.005
Erosion efficiency, γ, m/year $m^{1.5}$ $s^3/kg^{1.5}$	3×10^{-6}
Gravitational acceleration, g, m/s^2	9.8
Kinematic viscosity of the water, v, m^2/s	10^{-6}
Manning coefficient, n, –	0.034
Porosity, φ, –	0.2
Particle size, d, m	0.01
Ratio between width and depth, W_c/H, –	20
Threshold shear stress, τ_c, kg/m s^2	4.3

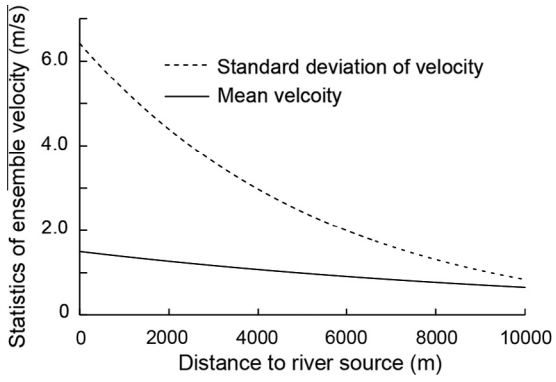

Fig. 4. The mean and variance of the ensemble velocity reducing streamwise.

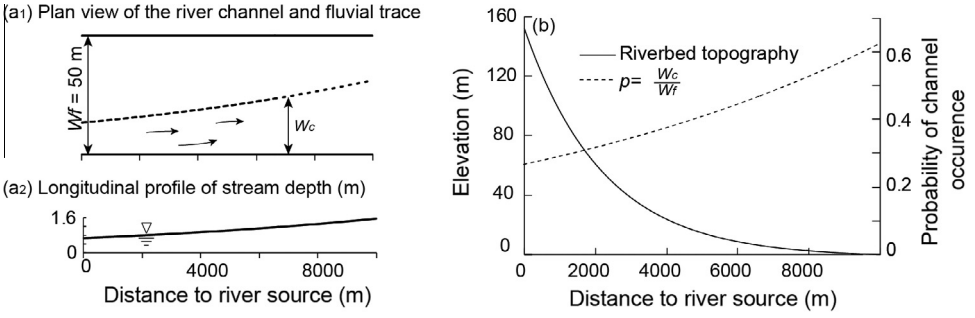

Fig. 3. (a) The spatial distribution of river width and depth for a river discharge of 50 m^3/s and (b) the riverbed topography and the probability of the channel occurrence at a position in the fluvial trace (P).

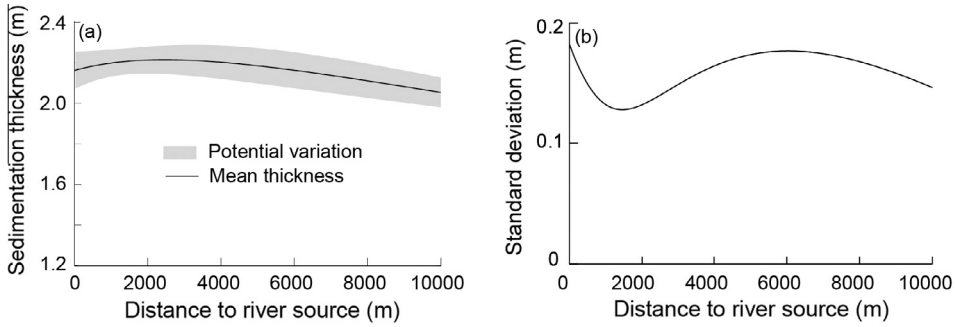

Fig. 5. (a) Sediment thickness and variation and (b) non-monotonic distribution of the standard deviation of sediment thickness compared to location in river system.

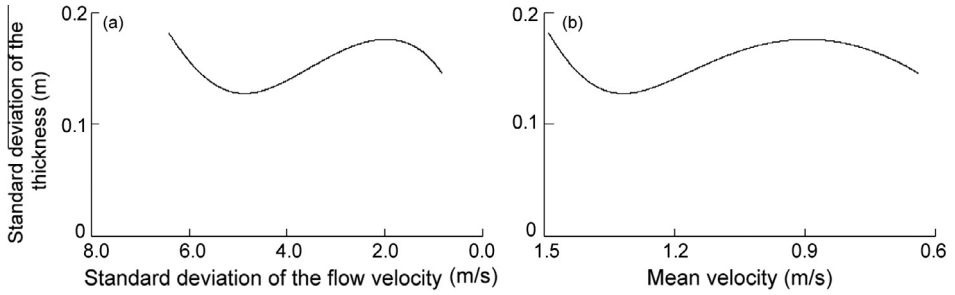

Fig. 6. Non-monotonic distribution of the standard deviation of sediment thickness versus (a) standard deviation and (b) mean of ensemble velocity.

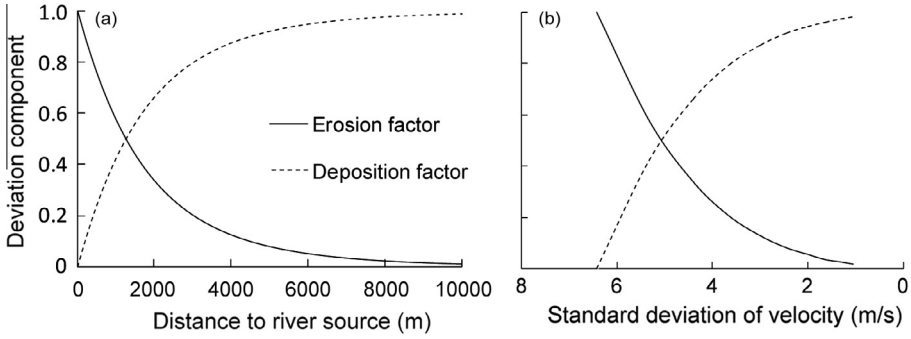

Fig. 7. (a) Streamwise perturbation of sediment thickness induced by the erosion and deposition processes and (b) their relationships with the standard deviation of velocity.

the decreases of $\bar{v}$ and σ_v^2 (according to Eq. (B5)). f_D increases streamwise, and also appears to increase with the decrease of σ_v. However, the increase in f_D is due to η' (or σ_η^2) being accumulated along the river flow (Eq. (21) and (B10)), rather than the direct stimulation of the velocity perturbation.

As shown in Fig. 8, the coupled processes of deposition and erosion in Fig. 7 contribute to a complex pattern of σ_z/σ_v (according to Eq. (28)), which decreases in the upstream area of the river. After σ_z/σ_v reaches the lowest value at a position around 1500 m, it increases further downstream (Fig. 8a). Because trends of σ_z/σ_v

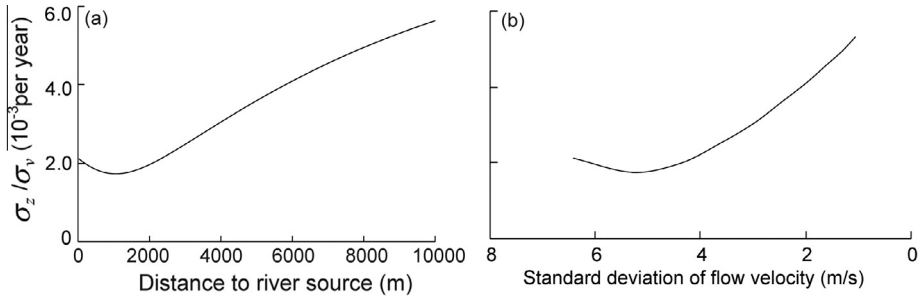

Fig. 8. The resultant thickness perturbation per standard deviation of flow velocity varying non-monotonically in the river flow direction.

and σ_v are opposite in the downstream part (when σ_v becomes smaller than 5 m/s, and the distance to the river source becomes larger than 1500 m) (Figs. 8b and 4), the resultant σ_z in Fig. 5b decreases again after a peak at about 6000 m.

Here we use an example with the statistics of velocity deceasing downstream, which results in a non-monotonic pattern of the sedimentation thickness due to the reverse roles played by the deposition and erosion processes. If the velocity statistics increase downstream, the non-monotonic sedimentation thickness pattern still appears. The statistics of the velocity can be much more complex than that used in this synthetic case, which either increase or decrease streamwise. To define the statistics of the velocity, geophysical approaches could be helpful to measure the shape of the fluvial trace, as well as long-term monitoring of the river flow rate.

6. Conclusion

Fluvial processes are affected by multiple geological and hydrological factors, including riverbed slope, river discharge and river channel position. Although these factors are difficult to determine in paleo-environments and are therefore uncertain, they can be related to paleo-flow velocity and quantified in a fluvial process model. In this paper, we developed a 1D stochastic fluvial process model (SFPM) based on the convective Exner equation by employing the perturbation method and the non-stationary spectral approach. The model avoids the detailed representation and simulation of stream velocity and channel evolution. Instead, velocity in the fluvial process model is defined as a mean value and a perturbation surrounding the mean. The sediment load and sedimentation thickness are expressed as functions of the statistics of velocity, where the statistics of velocity can be calculated, for example, simply based on the Manning equation.

The major contribution lies in coupling the statistics (mean and variance) of the flow velocity in a SFPM, which represent the influence of velocity fluctuation on resulting fluvial processes.

The SFPM predicts the mean and variance of sediment load in the river, and sediment thickness on the riverbed. Its applicability is demonstrated on a synthetic example, where the parameters are inferred from present-day analogue sites. The resultant sediment thickness and its variance follow non-monotonic patterns in space attributed to both erosion and deposition processes.

Acknowledgments

Funding support for this study came from China Scholarship Council and Queensland University of Technology, additional financial support from Exoma Energy Ltd is also gratefully acknowledged. Professor Chris Fielding is thanked for his constructive suggestions on conceptualizing the sedimentology environment. Daniel Owen and Matthias Raiber are thanked for proofreading.

Appendix A

The stochastic fluvial processes model in Section 2.2 uses the mean and variance (perturbation) of the velocity as key input parameters, which can represent the uncertainties in river discharge, riverbed slope and the position of the river channel in the fluvial trace. The evaluation of the velocity statistics from the uncertain geological and hydrological environments depends on data availability. This section presents a methodology to infer statistics of the velocity based on the Manning formula (e.g. Lague, 2010; Le Méhauté, 1976):

$$v_c(x,t) = \frac{c_f}{n(x,t)} R(x,t)^{\frac{2}{3}} S(x,t)^{\frac{1}{2}} = \frac{Q(x,t)}{A(x,t)}. \tag{A1}$$

Here v_c is the average stream velocity on the cross-section of the river channel perpendicular to the river flow direction (hereafter referred to as the Manning velocity), c_f is a conversion factor ($L^{1/3}/T$), n is the Manning coefficient, S is the riverbed slope, R is the hydraulic radius of the river channel (L), Q is the river discharge (L^3/T) and A is the wet area (L^2).

A1. Statistics of v relating to S and Q

The S of the river that led to the deposition of a geological formation can be inferred from lithology logs, which record the elevation of top and bottom of the formation. Q is commonly inferred by present-day analogues. In this study, we assume that the probability distributions of both S and Q at each position have been determined, possible values of S and Q are drawn from these probability distributions, and substituted into Eq. (A1) to generate realizations of v. We here assume the river channel shape to be quadrilateral (although other shapes are possible):

$$R(x,t) = \frac{W_c(x,t)H(x,t)}{W_c(x,t) + 2H(x,t)}, \quad A(x,t) = W_c(x,t)H(x,t), \tag{A2}$$

and the relationship between Q and W_c to satisfy (Viparelli et al., 2011):

$$\frac{W_c(x,t)}{W_{ref}} = \left[\frac{Q(x,t)}{Q_{ref}}\right]^{\alpha}, \tag{A3}$$

or between W_c and H (Parker et al., 1998):

$$\frac{W_c(x,t)}{H(x,t)} = \alpha. \tag{A4}$$

Here W_c is the width of the river channel (L), H is the depth of the river flow (L), α is a constant, and Q_{ref} and W_{ref} are the reference river discharge and the reference river channel width corresponding to Q_{ref}, respectively.

The statistics of v_c ($\bar{v}_c$ and $\sigma^2_{v_c}$) are then calibrated from the realizations. Uncertainty in parameters such as the manning coefficient n and the constant α can be considered in a similar fashion in $\bar{v}_c$ and $\sigma^2_{v_c}$.

A2. Statistics of v relating to channel movement

Another factor affecting v is channel movement. We consider channel movement as an uncertainty in the river channel location, which is defined as the probability of channel occurrence at a position of interest in the fluvial trace. Assuming that the channel has an equal probability of passing at each position on the cross-section of a fluvial trace perpendicular to the river flow direction, we obtain:

$$p(x,t) = \frac{W_c(x,t)}{W_f(x)}, \tag{A5}$$

where p is the probability of a channel occurrence ($p > 0$), W_f is the width of the fluvial trace, which can be surveyed by geophysical methods such as seismic survey, airborne electromagnetic surveys and remote sensing (e.g. Jin et al., 2011; Montgomery and Morrison, 1999; Vrbancich, 2009), and W_c can be determined from Eqs. A1, A2, A3, A4. If the river channel does not move within the simulation period, $p = 1$.

p is included in the statistics of v by assuming that when the channel does not pass through the position of interest, then v is zero at this position. When the channel passes through this position, the variability of v is induced by Q and S in the river channel (Section A1).

As a consequence (Appendix D),

$$\bar{v}(x,t) = p(x,t) \cdot \bar{v}_c(x,t), \tag{A6}$$

and

$$\sigma_v^2(x,t) = p(x,t)\sigma_{v_c}^2(x,t) + [1-p(x,t)][2-p(x,t)]\bar{v}_c^2(x,t), \tag{A7}$$

where $\bar{v}$ and σ_v^2 in Eqs. (A6) and (A7) are the ensemble mean and variance of velocity used in this study, and $\bar{v}_c$ and $\sigma_{v_c}^2$ are the mean and variance of velocity in the river channel.

Appendix B

The velocity is a key parameter, which affects the sediment transport and accumulation via altering the erosion and deposition rates. This section incorporates velocity statistics in the expressions of erosion and deposition rates.

B1. Erosion rate

A widely used expression for the erosion rate is given as (e.g. Lague et al., 2005; Tucker, 2004):

$$E = \gamma(\tau^{3/2} - \tau_c^{3/2}), \quad \tau > \tau_c, \tag{B1}$$

where γ is the erosion efficiency ($L^{2.5}\,T^2/M^{1.5}$), τ is the shear stress ($M/L\,T^2$) and τ_c is the critical shear stress above which the erosion starts. τ_c depends on river bed lithology which is calculated as (Cornelis et al., 2004):

$$\tau_c = k_t(\rho_s - \rho_f)gd, \tag{B2}$$

where k_t is dimensionless shear parameter, ρ_s is the dry density of sediments (M/L^3), and ρ_f is the density of water (M/L^3), d is the grain size of sediments (L), g is the gravitational acceleration (L/T^2).

As this study derives the stochastic fluvial process-based model by introducing the statistics of velocity, Eq. (B2) is here rewritten as a function of velocity.

The shear stress and stream velocity satisfy (Dade and Friend, 1998):

$$\tau = c_d\rho_f v^2, \tag{B3}$$

where c_d is the dimensionless drag coefficient.

Substituting Eq. (B3) in Eq. (B2) and making use of perturbation theory (Eq. (5)), the erosion rate is separated as a mean:

$$\bar{E} = \gamma[(c_d\rho_f)^{1.5}(\bar{v}^2 + 3\sigma_v^2)\bar{v} - \tau_c^{1.5}], \tag{B4}$$

and a perturbation:

$$E' = w_e v', \tag{B5}$$

where $w_e = \gamma(c_d\rho_f)^{1.5}(3\bar{v}^2 + \sigma_v^2)$.

B2. Deposition rate

The deposition rate is calibrated as (e.g. Davy and Lague, 2009; Winterwerp and Van Kesteren, 2004):

$$D = \beta\frac{\eta}{H}, \tag{B6}$$

where $\frac{\eta}{H}$ is depth-averaged concentration (L^3/L^3) and β is the deposition coefficient (L/T) relating to the settling velocity (ε_s) and vertical sediment concentration distribution:

$$\beta = k_d\varepsilon_s, \tag{B7}$$

Here, the vertical sediment concentration distribution is not simulated, its influence on D is represented by a concentration coefficient k_d. ε_s is the settling velocity of the particles (L/T), which relates to fluid and sediment properties (Dade and Friend, 1998):

$$\begin{aligned} \varepsilon_s &= \frac{gd^2}{18v}\frac{\rho_s-\rho_f}{\rho_f} \text{ for } d < 1 \text{ mm}, \\ \varepsilon_s &= \sqrt{gd\frac{\rho_s-\rho_f}{\rho_f}} \text{ for } d \geqslant 1 \text{ mm}, \end{aligned} \tag{B8}$$

where v is the kinematic viscosity of water (L^2/T).

Making use of Eq. (5) in Eq. (B6) results in the mean of deposition rate:

$$\bar{D} = \frac{\beta}{H_c}\bar{\eta}, \tag{B9}$$

and the perturbation

$$D' = \frac{\beta}{H_c}\eta', \tag{B10}$$

It is noted that D' in Eq. (8) indicates the influence of v' on η' via altering D. As D is unrelated to the stream velocity directly (Eq. (B6)), $D' = 0$. In contrast, η' feeds back into D, which then affects sediment thickness in Eq. (26). Therefore, D' is nonzero in estimates of σ_z^2, and is given by Eq. (B10).

Appendix C

The first order partial differential Eq. (15) subject to Eq. (17) can be solved as Cauchy problem, which converts Eq. (15) to (Hadamard, 2003):

$$\frac{dt}{1} = \frac{dx_k}{\bar{v}_k} = \frac{d\phi(x_k,t,\kappa)}{w_{uk}e^{i\kappa x_k}}. \tag{C1}$$

$\phi(x_k,t,\kappa)$ in Eq. (C1) is solved subject to spatial boundary condition (Eq. (17)) rather than a temporal initial condition. At the end of the first segment,

$$\phi(x_1,t,\kappa) = \frac{w_{u1}}{\bar{v}_1}\frac{1}{i\kappa}e^{i\kappa x_1} - \frac{w_{u1}}{\bar{v}_1}\frac{1}{i\kappa}. \tag{C2}$$

This study is based on a convective Exner equation, which represents the single-direction influence (Jost, 2012). This means that in a given river segment, the sediment load is only affected by river flow from upstream segments. For each segment, Eq. (C1) is solved subject to the boundary condition at the beginning of this segment, that is, $\phi(x_1,t,\kappa)$ at the end of first segment can be considered as the boundary condition for sediment transport in the second segment, and so on. Therefore, $\phi(x,t,\kappa)$ at the end of the second segment can be expressed as:

$$\phi(x_2,t,\kappa) = \frac{w_{u2}}{\bar{v}_2}\frac{1}{i\kappa}e^{i\kappa(x_2-x_1)} + \frac{w_{u1}}{\bar{v}_1}\frac{1}{i\kappa}e^{i\kappa x_1} - \left(\frac{w_{u1}}{\bar{v}_1}\frac{1}{i\kappa} + \frac{w_{u2}}{\bar{v}_2}\frac{1}{i\kappa}\right). \tag{C3}$$

Similarly, we can write $\phi(x,t,\kappa)$ at the end of the m-th segment as:

$$\phi(x_m,t,\kappa) = \frac{w_{um}}{\bar{v}_m}\frac{1}{i\kappa}e^{i\kappa(x_m-x_{m-1})} + \frac{1}{i\kappa}\sum_{k=1}^{m-1}\left(\frac{w_{uk}}{\bar{v}_k}\right)e^{i\kappa(x_k-x_{k-1})} - \frac{1}{i\kappa}\sum_{k=1}^{m}\left(\frac{w_{uk}}{\bar{v}_k}\right). \tag{C4}$$

The entire river is discretised into N segments with equal separation distance so that $\Delta x_k = x_k - x_{k-1}$ is a constant larger than zero. Therefore, we can write a general solution for $\phi(x,t,\kappa)$ at each node m as:

$$\phi(x_m,t,\kappa) = \left(\frac{1}{i\kappa}e^{i\kappa\Delta x} - \frac{1}{i\kappa}\right)\sum_{k=1}^{m}\left(\frac{w_{uk}}{\bar{v}_k}\right), \tag{C5}$$

where m is the index of node, $m = 0, 1, 2, \ldots N$.

Appendix D

The possible velocity in the river channel is given as the vector:

$$\mathbf{Vc} = [\dot{v}_1, \dot{v}_2, \dot{v}_3, \ldots \dot{v}_{n_1}], \tag{D1}$$

where n_1 is the size of the vector, and $\dot{v}_i$ are the possible values of stream velocity in the river channel ($i = 1, 2, \ldots n_1$).

The ensemble velocity vector is composed by the velocity in the river channel (river flowing through the position of interest) and zero (river channel does not pass at the position):

$$\mathbf{V} = [\dot{v}_1, \dot{v}_2, \dot{v}_3, \ldots \dot{v}_{n_1}, 0, 0..0]. \tag{D2}$$

The size of $\mathbf{V}$ is $n_1 + n_2$ and n_2 is the number of zero velocity, and the ratio between n_1 and $n_1 + n_2$ is the probability of channel occurrence, which is defined as the ratio between the width of river channel and fluvial trace:

$$p = \frac{n_1}{n_1 + n_2} = \frac{W_c}{W_f}. \tag{D3}$$

where W_c is the channel width and W_f is the width of fluvial trace.

The statistics of flow velocity in the river channel can be written as:

$$\bar{v}_c = \frac{1}{n_1}\sum_{i=1}^{n_1}\dot{v}_i, \sigma^2_{v_c} = \frac{1}{n_1}\sum_{i=1}^{n_1}(\dot{v}_i - \bar{v}_c)^2. \tag{D4}$$

where $\bar{v}_c$ and $\sigma^2_{v_c}$ are the mean and variance of flow velocity in the river channel, respectively.

Moreover, the mean and variance of the ensemble velocity in Eq. (D2) are:

$$\bar{v} = \frac{1}{n_1 + n_2}\left(\sum_{i=1}^{n_1}\dot{v}_i + \sum_{i=n_1+1}^{n_1+n_2} 0\right) = p \cdot \bar{v}_c, \tag{D5}$$

$$\sigma^2_v = \frac{1}{n_1 + n_2}\left[\sum_{i=1}^{n_1}(\dot{v}_i - p\bar{v}_c)^2 + \sum_{i=n_1+1}^{n_1+n_2}(p\bar{v}_c)^2\right], \tag{D6}$$

Eq. (D6) is further developed as follows:

$$\begin{aligned}\sigma^2_v &= \frac{1}{n_1 + n_2}\left[\sum_{i=1}^{n_1}[\dot{v}_i - \bar{v}_c + (1-p)\bar{v}_c]^2 + \sum_{i=n_1+1}^{n_1+n_2}(p\bar{v}_c)^2\right] \\ &= \frac{1}{n_1 + n_2}\left[n_1\sigma^2_{v_c} + 2(1-p)\bar{v}_c\left[\sum_{i=1}^{n_1+n_2} v'_i - \sum_{i=n_1+1}^{n_1+n_2}(0 - \bar{v}_c)\right]\right. \\ &\quad \left. + \sum_{i=1}^{n_1}(1-p)^2\bar{v}_c^2 + \sum_{i=n_1+1}^{n_1+n_2}(p\bar{v}_c)^2\right].\end{aligned} \tag{D7}$$

Considering that

$$E(v') = \frac{1}{n_1}\sum_{i=1}^{n_1+n_2} v'_i = 0, \tag{D8}$$

Eq. (D7) can then be written as:

$$\begin{aligned}\sigma^2_v &= \frac{1}{n_1 + n_2}\left[n_1\sigma^2_{v_c} + 2(1-p)\bar{v}_c \cdot n_2\bar{v}_c + n_1(1-p)^2\bar{v}_c^2 + n_2(p\bar{v}_c)^2\right] \\ &= p\sigma^2_{v_c} + (1-p)(2-p)\bar{v}_c^2.\end{aligned} \tag{D9}$$

References

Cornelis, W.M., Gabriels, D., Hartmann, R., 2004. A parameterisation for the threshold shear velocity to initiate deflation of dry and wet sediment. Geomorphology 59 (1), 43–51.

Cox, D.R., Hinkley, D.V., 1979. Theoretical Statistics. CRC Press, 511 pp.

Cui, Y. et al., 2003. Sediment pulses in mountain rivers: 1. Experiments. Water Resour. Res. 39 (9), 1239.

Dade, W.B., Friend, P.F., 1998. Grain-size, sediment-transport regime, and channel slope in alluvial rivers. J. Geol. 106 (6), 661–676.

Dagan, G., 1989. Flow and Transport in Porous Formations. Springer-Verlag.

Davy, P., Lague, D., 2009. Fluvial erosion/transport equation of landscape evolution models revisited. J. Geophys. Res.: Earth Surf. (2003–2012), 114, F3

Exner, F.M., 1925. Uber die wechselwirkung zwischen wasser und geschiebe in flüssen. Sitzungsber. Akad. Wiss. Wien Abt. IIa 134, 166–204.

Furbish, D.J., Haff, P.K., Roseberry, J.C., Schmeeckle, M.W., 2012. A probabilistic description of the bed load sediment flux: 1. Theory. J. Geophys. Res.: Earth Surf. (2003-2012), 117, F3

Gelhar, L.W., Axness, C.L., 1983. Three-dimensional stochastic analysis of macrodispersion in aquifers. Water Resour. Res. 19 (1), 161–180.

Gibbs, J.W., 2010. Elementary Principles in Statistical Mechanics: Developed with Especial Reference to the Rational Foundation of Thermodynamics. Cambridge University Press.

Gonzalez-Juez, E., Meiburg, E., Constantinescu, G., 2009. Gravity currents impinging on bottom-mounted square cylinders: flow fields and associated forces. J. Fluid Mech. 631, 65.

Hadamard, J., 2003. Lectures on Cauchy's Problem: In Linear Partial Differential Equations. DoverPublications. com.

Holmes, M.H., 2013. Introduction to Perturbation Methods, 20. Springer.

Jin, S., Feng, G., Gleason, S., 2011. Remote sensing using GNSS signals: current status and future directions. Adv. Space Res. 47 (10), 1645–1653.

Jost, J., 2012. Partial Differential Equations. Springer, Dordrecht.

Koltermann, C.E., Gorelick, S.M., 1992. Paleoclimatic signature in terrestrial flood deposits. Science 256 (5065), 1775–1782.

Koltermann, C.E., Gorelick, S.M., 1996. Heterogeneity in sedimentary deposits: a review of structure-imitating, process-imitating, and descriptive approaches. Water Resour. Res. 32 (9), 2617–2658.

Lague, D., 2010. Reduction of long-term bedrock incision efficiency by short-term alluvial cover intermittency. J. Geophys. Res.: Earth Surf. (2003-2012), 115, F2

Lague, D., 2014. The stream power river incision model: evidence, theory and beyond. Earth Surf. Process. Landforms 39 (1), 38–61.

Lague, D., Hovius, N., Davy, P., 2005. Discharge, discharge variability, and the bedrock channel profile. J. Geophys. Res.: Earth Surf. (2003-2012), 110, F4

Lanzoni, S., Seminara, G., 2002. Long-term evolution and morphodynamic equilibrium of tidal channels. J. Geophys. Res.: Oceans (1978–2012), 107(C1), 1-1-1-13.

Le Méhauté, B., 1976. An Introduction to Hydrodynamics and Water Waves. Springer-Verlag, New York.

Leliavsky, S., 1955. An introduction to fluvial hydraulics. Constable London.

Lesshafft, L., Meiburg, E., Kneller, B., Marsden, A., 2011. Towards inverse modeling of turbidity currents: the inverse lock-exchange problem. Comput. Geosci. 37 (4), 521–529.

Li, F., Dyt, C., Griffiths, C., 2004. 3D modelling of flexural isostatic deformation. Comput. Geosci. 30 (9), 1105–1115.

Li, S.-G., McLaughlin, D., 1995. Using the nonstationary spectral method to analyze flow through heterogeneous trending media. Water Resour. Res. 31 (3), 541–551.

Molnar, P., Anderson, R.S., Kier, G., Rose, J., 2006. Relationships among probability distributions of stream discharges in floods, climate, bed load transport, and river incision. J. Geophys. Res.: Earth Surf. (2003-2012), 111, F2

Montgomery, S.L., Morrison, E., 1999. South Eubank Field, Haskell County, Kansas; a case of field redevelopment using subsurface mapping and 3-D seismic data. AAPG Bull. 83 (3), 393–409.

Necker, F., Hartel, C., Kleiser, L., Meiburg, E., 2005. Mixing and dissipation in particle-driven gravity currents. J. Fluid Mech. 545, 339–372.

Ni, C.-F., Li, S.-G., Liu, C.-J., Hsu, S.M., 2010. Efficient conceptual framework to quantify flow uncertainty in large-scale, highly nonstationary groundwater systems. J. Hydrol. 381 (3), 297–307.

Paola, C., 2000. Quantitative models of sedimentary basin filling. Sedimentology 47 (s1), 121–178.

Paola, C., Heller, P.L., Angevine, C.L., 1992. The large-scale dynamics of grain-size variation in alluvial basins, 1: Theory. Basin Res. 4 (2), 73–90.

Paola, C., Voller, V., 2005. A generalized Exner equation for sediment mass balance. J. Geophys. Res.: Earth Surf. (2003-2012), 110, F4

Parker, G., Paola, C., Whipple, K.X., Mohrig, D., 1998. Alluvial fans formed by channelized fluvial and sheet flow. I: Theory. J. Hydr. Eng. 124 (10), 985–995.

Roseberry, J.C., Schmeeckle, M.W., Furbish, D.J., 2012. A probabilistic description of the bed load sediment flux: 2. J. Geophys. Res.: Earth Surf. (2003–2012), 117, F3

Simpson, G., Castelltort, S., 2006. Coupled model of surface water flow, sediment transport and morphological evolution. Comput. Geosci. 32 (10), 1600–1614.

Sklar, L.S. et al., 2009. Translation and dispersion of sediment pulses in flume experiments simulating gravel augmentation below dams. Water Resour. Res. 45 (8), W08439.

Tetzlaff, D.M., 1990. SEDO: a simple clastic sedimentation program for use in training and education. Quantitative Dynamic Stratigraphy. Prentice-Hall, Englewood Cliffs, New Jersey, pp. 401–415.

Tucker, G.E., 2004. Drainage basin sensitivity to tectonic and climatic forcing: Implications of a stochastic model for the role of entrainment and erosion thresholds. Earth Surf. Process. Landforms 29 (2), 185–205.

Tucker, G.E., Bras, R.L., 2000. A stochastic approach to modeling the role of rainfall variability in drainage basin evolution. Water Resour. Res. 36 (7), 1953–1964.

Van De Wiel, M.J., Coulthard, T.J., Macklin, M.G., Lewin, J., 2011. Modelling the response of river systems to environmental change: progress, problems and

prospects for palaeo-environmental reconstructions. Earth Sci. Rev. 104 (1–3), 167–185.
Viparelli, E., Gaeuman, D., Wilcock, P., Parker, G., 2011. A model to predict the evolution of a gravel bed river under an imposed cyclic hydrograph and its application to the Trinity River. Water Resour. Res. 47 (2).
Voller, V.R., Ganti, V., Paola, C., Foufoula-Georgiou, E., 2012. Does the flow of information in a landscape have direction? Geophys. Res. Lett. 39 (1).
Vrbancich, J., 2009. An investigation of seawater and sediment depth using a prototype airborne electromagnetic instrumentation system–a case study in Broken Bay, Australia. Geophys. Prospect. 57 (4), 633–651.
Winterwerp, J.C., Van Kesteren, W.G., 2004. Introduction to the Physics of Cohesive Sediment Dynamics in the Marine Environment. Elsevier.
Zhu, J., Satish, M., 1999. Stochastic analysis of macrodispersion in a semi-confined aquifer. Trans. Porous Media 35 (3), 273–297.
Zolezzi, G., Seminara, G., 2001. Downstream and upstream influence in river meandering. Part 1. General theory and application to overdeepening. J. Fluid Mech. 438, 183–211.